



Rock mechanical failure characteristics and energy evolution analysis of coal-rock combination with different dip angles

Wenbing Shen¹ · Weijian Yu^{1,2} · Bao Pan¹ · Ke Li^{1,3}

Received: 6 February 2021 / Accepted: 8 December 2021 / Published online: 4 January 2022
© Saudi Society for Geosciences 2021

Abstract

Given the roadway deformation and surrounding rock control in the process of thin coal seam mining, the coal-rock combination with inclination angles for 0°, 15°, 30°, 45°, and 60° was designed. The rock mechanic test machine was used to conduct a uniaxial compression test and a graded loading and unloading test on the coal-rock combination; the failure characteristics of the two were compared and analyzed. The stress–strain data obtained by the experiment is plotted by Origin software. On the basis of the obtained curve, energy density is integrated and the energy density data is fitted. The results show that ultimate compressive strength of coal-rock combination under uniaxial loading is higher than that under cyclic loading and unloading. The failure of uniaxial primary loading mainly presents a single shear failure mode, while the coal and rock mass present X-type shear failure mode under graded loading and unloading, which makes the coal body more break. From the energy density curve, it can be observed that with the increase of inclination angle, the ultimate compressive strength of the coal-rock combination decreases, and its input Li energy and elastic energy also decreases, and the dissipation dissipates faster. In the follow-up research process, the deformation characteristics of coal and rock mass with a large dip angle will continue to research roadway support stability. The adaptability of roadway support provides a reference for roadway support engineering of coal and rock with large dip angle, which has a specific reference value.

Keywords Rock mechanics · Rock-coal-rock combination · Inclined angle · Cyclic loading and unloading · Energy evolution

Introduction

Due to the differences in mechanical properties of coal and rock, inconsistent deformation characteristics will appear. Therefore, to analyze the failure characteristics and

mechanical analysis of coal-rock combinations under different conditions with dip angle (Zhao and Zhao 2018) most scholars in China and abroad used coal-rock combination samples for rock mechanics laboratory tests. At present, the study focus on the mechanical properties and failure modes of different inclination combinations such as 0°, 15°, 30°, 45°, and 60°. The variation characteristics of energy under the condition of graded loading and unloading can provide a theoretical basis for the mining of thin coal seam, then improve the mining scheme of mining areas according to the field geological conditions (Yu et al. 2018; Xie et al. 2012). The analysis of weak broken surrounding rock large dip angle was established in large dip angle mining and supported resistance between the intrinsic relationship (Qin et al. 2015). Based on numerical simulation, the model of large dip angle soft roof and floor is established, and the relationship between support and surrounding rock stress is analyzed to provide a theoretical basis for surrounding rock support technology under large dip angle fully mechanized mining (Shi et al. 2012). Through the establishment of

Responsible editor: Zeynal Abiddin Erguler

✉ Weijian Yu
ywjl@163.com

Wenbing Shen
1042477057@qq.com

¹ School of Resource and Environment and Safety Engineering, Hunan University of Science and Technology, Xiangtan 411201, China

² Hunan Provincial Key Laboratory of Safe Mining Techniques of Coal Mines, Hunan University of Science and Technology, Xiangtan 411201, China

³ College of Mining, Guizhou Institute of Technology, Guiyang 550003, Guizhou, China

numerical calculation models under different rock strata dip angles, the asymmetric failure mechanism of the coal-rock roadway with large dip angle is studied, and the asymmetric coupling support technology at key parts of roadway surrounding rock is proposed, which realizes the coordination between the support structure and surrounding rock (Zhang et al. 2011). The cyclic loading and unloading test of sandstone under pore water pressure was carried out to analyze the energy evolution law of input energy, elastic energy, and dissipation energy in the process of sandstone deformation (Xu et al. 2011).

The relationship between elastic energy and loading–unloading variation, the overall strength, and failure mechanism of the coal-rock combination are comprehensively analyzed by using the coal-rock combination (Zuo et al. 2011a, b, 2016). The relationship between energy density and stress curve is divided into three stages: slow growth, nonlinear growth, and post-peak drop stage. The input energy, elastic energy, and dissipation energy density increase with the increase of stress under graded loading and unloading, which offered the theoretical foundation for preventing and controlling coal mine disasters (Chen et al. 2017, 2018). A relatively complete and detailed analysis of the coal-rock interface with different dip angles was conducted; the failure characteristics and deformation characteristics of the coal-rock interface with different dip angles are explored. The anchor bolts' role and mechanism in the coal-rock-anchor composite anchorage are summarized (Yu et al. 2019a, b, c). The failure process, failure characteristics, and stress–strain characteristics of different coal and rock masses under uniaxial compression were studied, and the influence of mechanical strength on composite specimens' mechanical behavior was analyzed (Zhu et al. 2016). The evolution laws of input energy density, elastic energy density, dissipated energy density, elastic modulus, and uniaxial compressive strength of coal-rock combination under uniaxial and loading and unloading conditions were studied. The energy storage characteristics of different samples were obtained. Based on the mechanical response, energy evolution, and deformation failure characteristics of coal-rock combination, the energy

evolution law of coal-rock combination failure was established, and discussed (Yang et al. 2019).

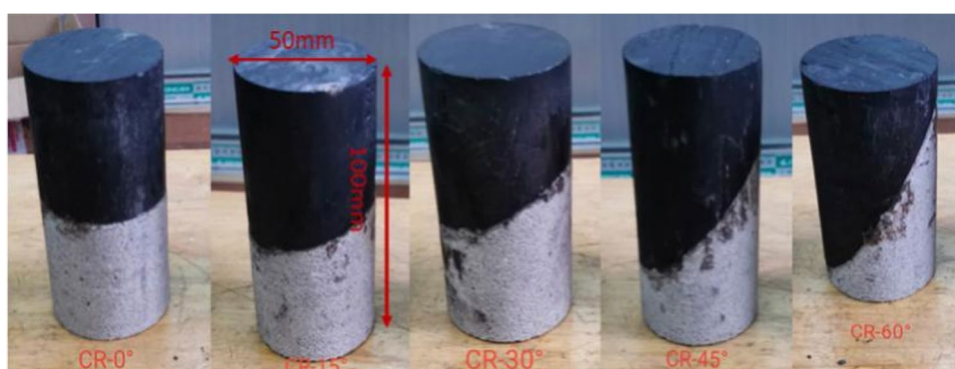
The above studies have mainly focused on the effect of cyclic loading and unloading on rock mass and coal mass. Many scholars have studied the mechanical behavior of a coal-rock combination structure under graded loading and unloading (Xu et al. 2006). The author carried out a detailed study on coal-rock mass with different dip angles combined with his ideas based on the previous studies. After studying basic mechanical behavior of coal-rock combination under uniaxial once loading, this paper will study the mechanical properties and energy evolution of coal-rock combination under cyclic loading, which is of great significance for scientific and reasonable understanding of roadway support design under the influence of repeated mining in the process of coal mining (Zheng et al. 2015).

Experimental summary

Fabrication of specimen

The coal and sandstone of the monomer and combination used in this experiment are obtained from a mining area in Hunan Province, China. The obtained sandstone and coal are processed and prepared by professional institutions. The specimens are strictly by the International Society of Rock Mechanics (ISRM) standard, and the height-diameter ratio is 2:1 to make a 50-mm diameter and 100-mm height, respectively. The inclined coal-rock combination in this experiment is composed of sandstone and coal-rock by contacting and bonding with a special engineering adhesive to form a combination specimen with different angles. The combination takes the radial line of sandstone and coal-rock as the axial center and is combined in a ratio of 1:1 to form coal-rock combination with 5 different dip angles of 0° , 15° , 30° , 45° , and 60° . Some specimens are shown in Fig. 1. The parallelism of each cylinder must be less than 0.02 mm. In order to reduce the error and discreteness of the experimental results, 5 specimens of each type were selected and the two specimens with

Fig. 1 Partially inclined coal-rock composite specimens



similar experimental results were used as the basis for the experimental results.

Test scheme and equipment

As shown in Fig. 2(a), the RMT-150C rock mechanics test system developed by the Wuhan Institute of Rock Mechanics, Chinese Academy of Sciences, was used to collect the specimen’s axial strain axial pressure automatically. Because this test equipment has only one set of axial sensors, it is impossible to simultaneously measure coal’s circumferential strain and rock mass of the combination. Therefore, two 120–10AA resistance strain gauges are affixed to the coal rock mass’ two same heights, respectively. The D3816N strain acquisition system automatically collects the measured values. The resulting uniaxial compressive test data are compared, as shown in Fig. 2(b).

Uniaxial cyclic loading and unloading were carried out on the coal-rock combination after the test preparation. Uniaxial cyclic loading and unloading were carried out on the coal-rock combination by the uniaxial compressive strength obtained by the loading test machine. Taking 5 kN as a cycle, each cycle increased by 5 kN compared with the previous cycle. In the whole cyclic loading process, the load control loading process and the load are controlled by oblique waveform + triangular waveform. This is to adjust the rate to 0.1 kN/S at the initial stage of cyclic loading. When the load is loaded to average value of the whole ultimate load, the load control mode is adjusted to triangular waveform, and the frequency is 0.001 Hz. When the load of coal-rock combination increases to the ultimate peak, it decreases to 5 kN and enters the next cycle until the final failure of coal-rock composite specimen.

Uniaxial test of coal-rock combination

As shown in Table 1, sandstone’s average compressive strength is 29.32 MPa, while that of the coal monomer is 21.72 MPa. Compared with sandstone, the compressive strength of the coal monomer is lower than that of sandstone. The reason may be that the coal body’s internal defects and looseness lead to low compressive strength.

The deformation and failure of the coal-rock combination after loading have gone through four stages (Qin et al. 2017): the compaction stage, elastic stage, plastic deformation stage, and post-peak failure stage are similar to the failure process of coal and sandstone specimens. For the coal-rock combination with 0° dip angle, its ultimate compressive

Table 1 Fundamental physicochemical parameters of coal-rock combination bodies under uniaxial compression tests

Category	Test specimen number	Uniaxial compressive strength (MPa)	Elastic modulus (GPa)
True coal	C-1	23.56	2.776
	C-2	19.89	2.493
Sandstone	R-1	27.35	7.829
	R-2	31.29	7.827
Dip angle 0°	CR-0°-1	27.34	5.289
	CR-0°-2	28.78	4.155
Dip angle 15°	CR-15°-1	26.17	3.700
	CR-15°-2	26.92	4.276
Dip angle 30°	CR-30°-1	23.23	3.094
	CR-30°-2	24.98	5.928
Dip angle 45°	CR-45°-1	19.01	3.163
	CR-45°-2	20.21	3.291
Dip angle 60°	CR-60°-1	16.78	3.647
	CR-60°-2	17.17	2.721

Fig. 2 Test equipment and strain gauges



(a) testing equipment

(b) resistance strain gauge

strength is higher, and the highest compressive strength is 28.78 MPa, which is higher than that of other dip angles. The coal-rock combination's uniaxial compressive strength with a dip angle of 15° is lower than that of 0°, and the maximum compressive strength is about 26.17 MPa. For coal-rock combination with a dip angle of 30° and 45°, the compressive strength decreases until the ultimate compressive strength reaches the minimum when the dip angle is 60°, and the slip phenomenon occurs while the shear failure occurs (Zuo et al. 2011a, b). Some specimens were crushed. It can be seen from the failure mode that failure of the combination is concentrated in the coal body. The integrity of the specimens with different inclination angles is significantly different after failure, as shown in Fig. 3.

Graded loading and unloading experiments of coal-rock assemblages with different dip angles

Graded loading and unloading stress and strain of inclined coal-rock combination

To analyze the effect of cyclic loading on coal and rock mass in the mining process, uniaxial graded loading and unloading experiments were carried out on coal and rock mass with different dip angles. The mechanical parameters in Table 2 of the experimental results show that under graded loading and unloading, the difference between the ultimate

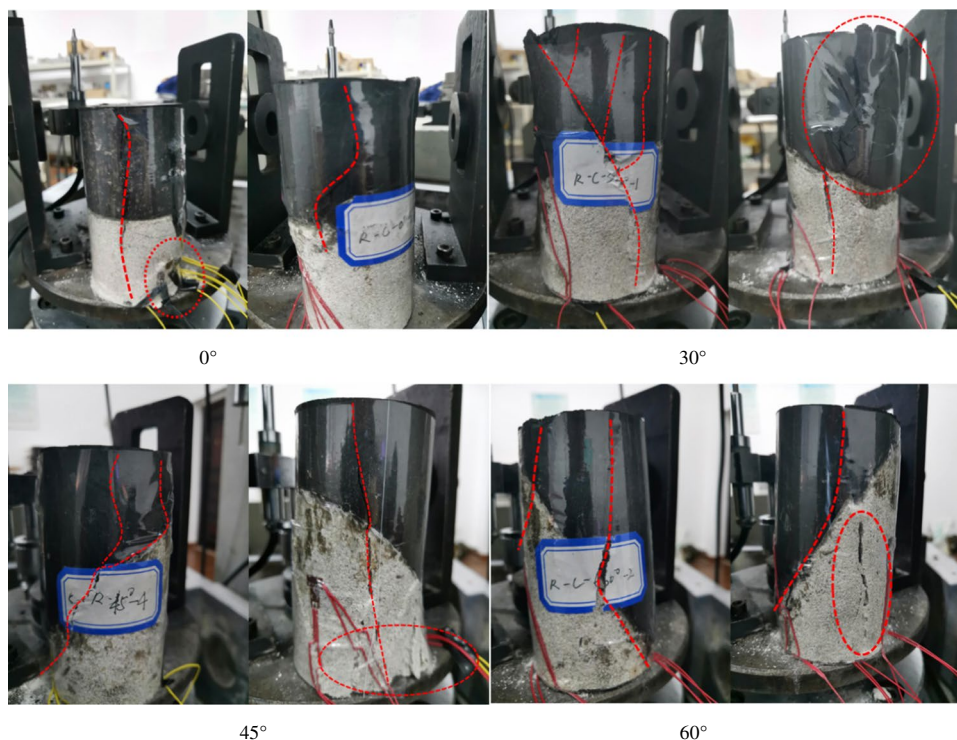
Table 2 Loading and unloading mechanical parameters of coal-rock combination with different dip angles

Category	Test specimen number	Uniaxial loading and unloading strength (MPa)	Elastic modulus (GPa)
Dip angle 0°	CR-0°-3	28.59	4.173
Dip angle 15°	CR-15°-4	27.72	6.728
Dip angle 30°	CR-30°-3	23.13	6.539
Dip angle 45°	CR-45°-4	17.52	4.217
Dip angle 60°	CR-60°-3	15.78	4.339

compressive strength of the coal-rock combination with an inclination angle $\leq 30^\circ$ and the compressive strength under uniaxial primary loading (Table 1) is small. When the inclination angle is above 45°, compressive strength of the combination decreases and the specimen with a 60° combination angle reaches minimum value (15.78 MPa). The main reason may be that during the graded loading and unloading process, the internal failure cracks continue to expand under cyclic disturbance, making the integrity of coal and rock mass destroyed and the strength reduced.

As shown in Fig. 4, each sample extracts a typical loading curve under the loading and unloading conditions of different cycles. From the stress–strain curve of the graded loading and unloading of the coal-rock combination, it can be seen that due to the loose and weak internal coal body, there are primary cracks, and due to the viscosity of the rock mass, the loading curve and the unloading curve of the coal-rock

Fig. 3 Typical damage characteristics under uniaxial compression tests



combination under a cycle do not coincide. Moreover, the last unloading curve does not coincide with the next loading curve, and the middle non-coincidence area forms a hysteresis loop (Xiao et al. 2014). Due to the significant difference in material between coal and rock mass, the internal mineral composition changes under the long-term change of natural environment, and many cracks, joints, holes, and other microstructure appear. Simultaneously, under long-term natural conditions, there is moisture and a small amount of gas inside, which is precise because of these significant characteristics that the cycle area does not coincide to form a hysteresis loop.

It can be seen from the curve in Fig. 4 that the curves of loading and unloading with inclination angles of 0° and 15° are approximate and have no noticeable change. However, the area of the hysteresis loop increases significantly when it reaches the sixth cycle. This is because the coal is gradual, and the coal is gradually destroyed under the action of pressure. The strain rate of coal failure is faster than that of the rock mass, and the axial strain generated after the overall failure increases. Compared with the inclination angle of 0°, the hysteresis loop with an inclination angle of 15° increases with the increase of cycles, and its axial strain increases faster than that of 0°. In contrast, the specimen’s plastic hysteresis loop with an inclination angle above 30° shifts to the right as a whole. The strain at the end of loading and unloading increases with the increase of loading times; that is, each cycle produces a certain amount of plastic deformation. The plastic deformation generated by the previous cycle is then attached to the plastic deformation generated by the subsequent cycle. Also, the release of elastic energy of coal and rock mass under each unloading will produce a small number of cracks and holes, and then continue to produce plastic deformation in the next cycle. The combination of an inclination angle of 60° is more obvious.

Mechanical failure analysis of inclined coal-rock combination

Since the mechanical properties of sandstone and coal are quite different, the coal-rock combination system will produce different deformations under load. Under the same load, the axial strain of sandstone at both ends of the composite is smaller than that of coal, and the high-strength engineering binder at the contact surface between rock mass and coal mass makes the composite not move wrong at the coal-rock contact surface. As shown in Fig. 5(a) schematic diagram, it can be seen that the upper and lower edges of the coal-rock interface (coal extrusion fragile area) have the greatest possibility of failure,

followed by the secondary stress superposition area of coal and rock mass. When the vertical force increases continuously, the stress superposition increases gradually until failure, forming a penetrating crack from coal to rock mass, and the failure is also increasing with the increasing inclination. Here, we assume that (1) the strength of coal-rock association follows the Mohr–Coulomb criterion, (2) the Mohr–Coulomb criterion of inclined coal-rock structural plane, and (3) the homogeneity of coal-rock association with dip angle.

As shown in Fig. 5(b), Mohr stress circle theory shows that the normal stress σ and shear stress τ of the contact surface of coal-rock combination with dip angle can be calculated by the first and third principal stresses (Cai 2013):

$$\begin{cases} \sigma = \frac{1}{2}(\sigma_1 + \sigma_3) + \frac{1}{2}(\sigma_1 - \sigma_3) \cos(2\beta) \\ \tau = \frac{1}{2}(\sigma_1 - \sigma_3) \sin(2\beta) \end{cases} \quad (1)$$

In the formula, σ_1 is the maximum principal stress of coal-rock combination that is axial stress, σ_3 is the minimum principal stress that is confining pressure stress, β is the angle of coal-rock interface and horizontal plane, and s and τ will increase with the increase of inclination angle.

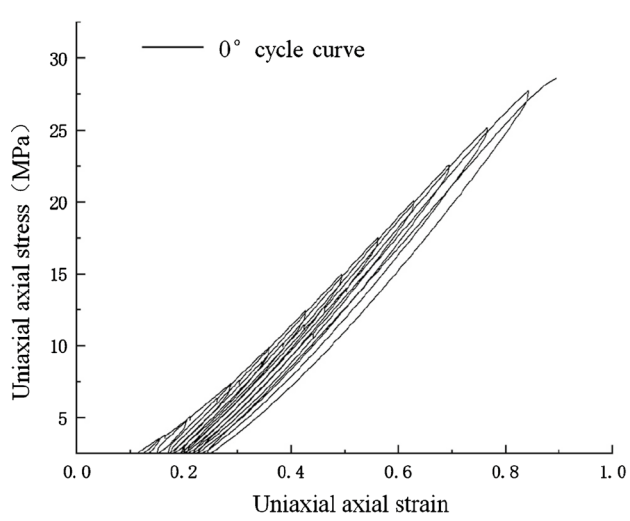
Assuming that the shear strength of structural planes between coal-rock assemblages obeys Coulomb criterion, there are

$$\tau = c + \sigma \tan \varphi \quad (2)$$

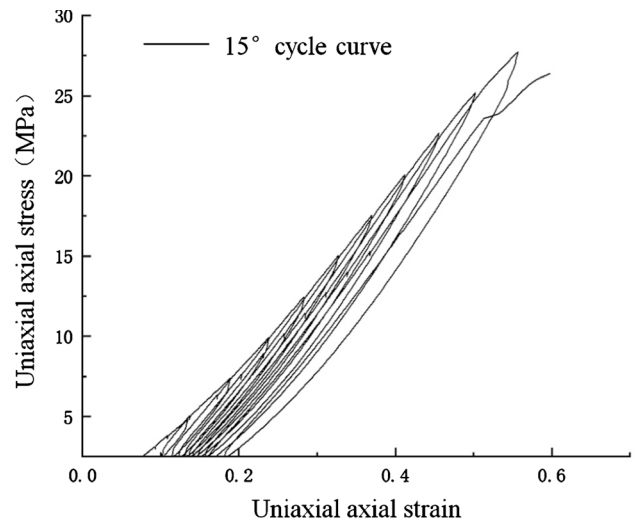
In the formula, $c = c_0, c_\omega$, and $\varphi = \varphi_0, \varphi_\omega$, where c_0, c_ω are the cohesion (MPa) of coal-rock combination system and coal-rock structural plane, respectively, and $\varphi_0, \varphi_\omega$ are the internal friction angle (°) of coal-rock combination system and coal-rock structural plane. By combining Eqs. (1) and (2), we can obtain

$$\sigma_1 = \sigma_3 + \frac{2(c_\omega + \sigma_3 \tan \varphi_\omega)}{(1 - \tan \varphi_\omega \cot \beta) \sin(2\beta)} \quad (3)$$

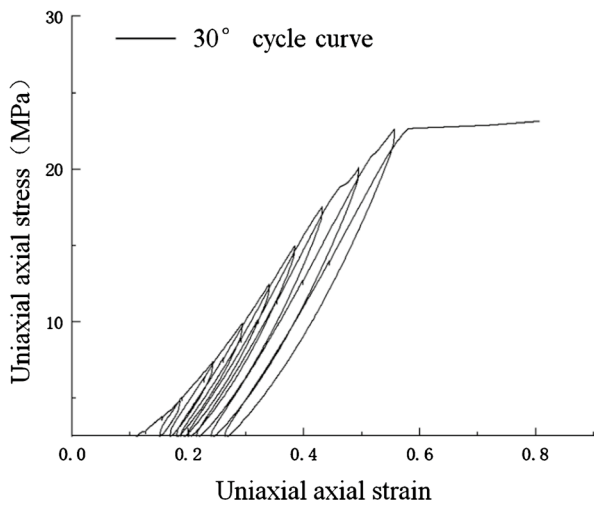
Formula (3) is the failure strength condition of the structural plane of the coal-rock combination. Because of the coal and rock materials used in this experiment, the cohesion and friction angle in this paper are just to follow the traditional concept to describe the overall properties of coal and rock, which is more characterized by the contact surface properties of coal and rock. For Eq. (3), c_ω and φ_ω are the internal friction angle of coal-rock structural plane. According to Mohr circle and envelope, β is the intersection angle between coal-rock structural plane and horizontal plane. The derived formula is only used for the



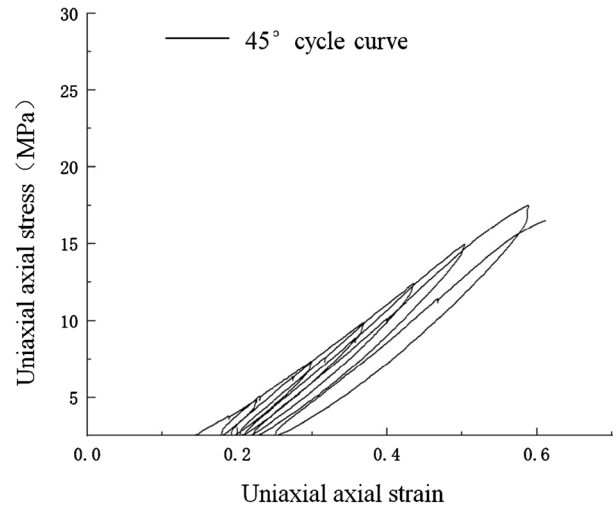
(1) Dip angle 0°



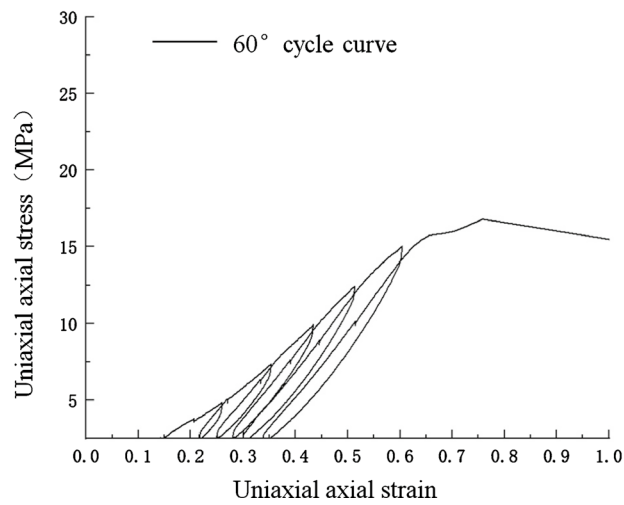
(2) Dip angle 15°



(3) Dip angle 30°



(4) Dip angle 45°



(5) Dip angle 60°

◀**Fig. 4** Deformation and failure diagrams with different dip angles under graded loading and unloading

coal-rock combination with dip angle, and the shear slip failure condition of coal-rock contact surface under the action of confining pressure.

Fig. 5 Mechanical model of composite specimens under compression

Graded loading and unloading failure characteristics of coal-rock assemblages with different dip angles

Some typical failure situations in the graded loading and unloading experiment of the coal-rock combination are shown in Fig. 5. From the typical failure characteristics of

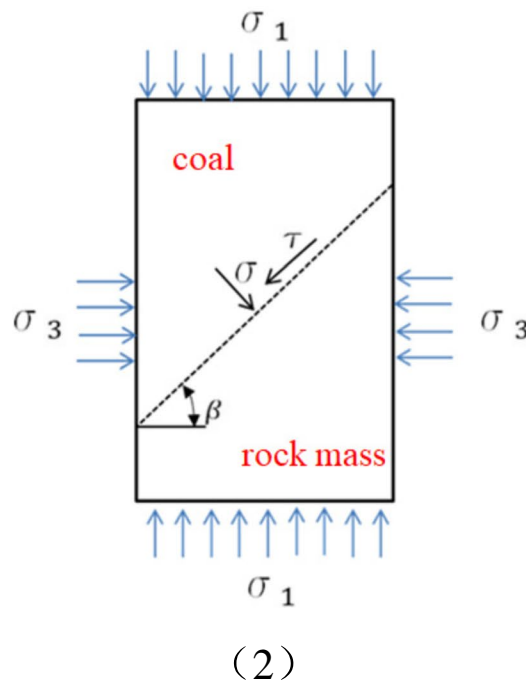
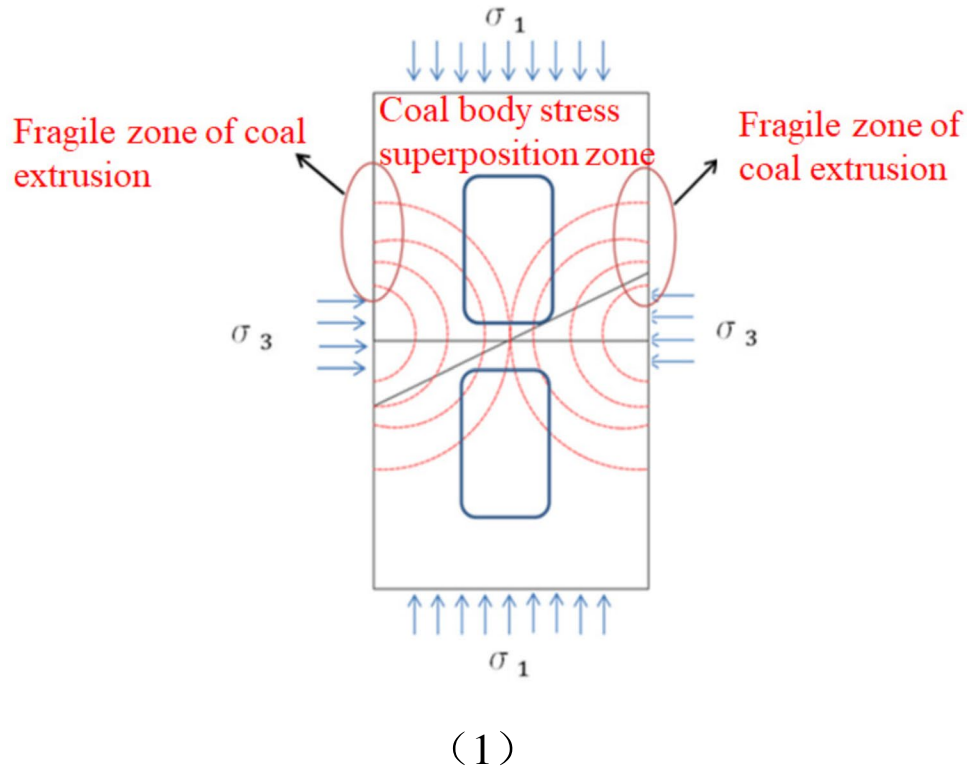


Fig. 5, the coal-rock combinations with different dip angles have undergone different failure degrees. However, the degree of failure of coal and rock is different, and partial failure of the coal body is more severe as a whole, showing X-shaped shear failure (such as Fig. 5 (30°)). However, the partial crushing of coal at 30° and 45° is more serious, and the crack distribution is dense. Compared with the uniaxial one-time loading failure, although the failure is a brittle shear failure, it is more complete than the uniaxial one-time loading coal crushing, mainly caused by the fatigue damage inside the coal body in the process of graded loading and unloading. From the failure states of dip angles of 30° and 60° in the figure, the main failure cracks in the coal part mostly run through the rock part, while the coal part's failure is large and concentrated.

Besides, the axial deformation and circumferential deformation have a significantly decreasing trend compared with the uniaxial one-time loading. The slip phenomenon of coal-rock combination with a dip angle of 60° is more obvious than that under uniaxial compression, and the cracks are more concentrated and concentrated at the interface between coal and rock mass. The test results show that the cyclic loading and unloading help the rapid expansion of cracks inside the composite, which reduces the overall strength of the composite. With the increase of dip angle, the broken degree of the coal part is more obvious, and the cracks are mostly concentrated in the coal-rock interface. The failure changes from single shear failure to a composite shear with an X shape. It can be seen from the partial failure

state of rock mass and the initial position of cracks that the main factors of rock mass failure may be the rapid expansion of cracks and the sudden release of elastic energy in the failure process of coal.

Energy evolution law of combination

Internal energy analysis of the combination

During the uniaxial cyclic loading and unloading experiment, the energy inside the system when the coal-rock combination is subjected to load is mainly divided into four processes: energy input, energy accumulation, energy dissipation, and energy release. During the compression process of coal and rock mass, the energy input of coal-rock combination is the work by the experimental machine on the specimen, in which part of the energy input to the system is stored in the form of elastic energy, and the rest is released in the form of internal failure and plastic deformation (Yang et al. 2019):

$$U = U_e + U_p \quad (4)$$

where U is the input energy (J), U_e is the released elastic energy (J), and U_p is for internal dissipation energy (J).

The experiment shows that the compressive strength of coal is far lower than the compressive strength of rock mass, and the linear elastic stage begins when the coal reaches ultimate failure strength. Therefore, it can be considered that in

Fig. 6 Typical damage characteristics of coal and rock masses with different dip angles under staged loading and unloading

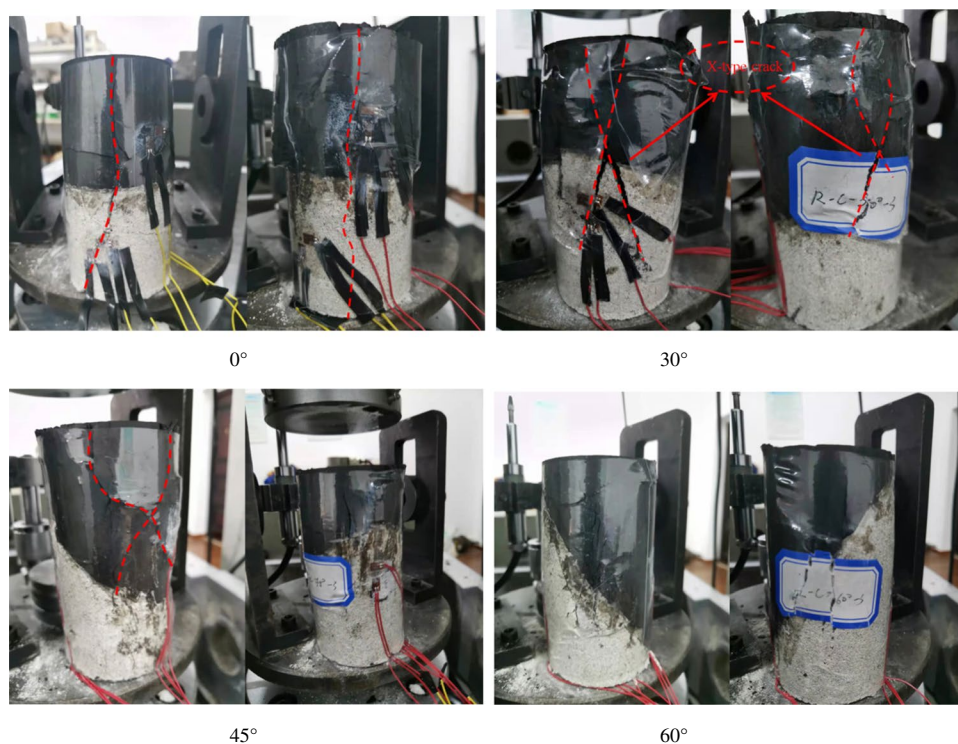
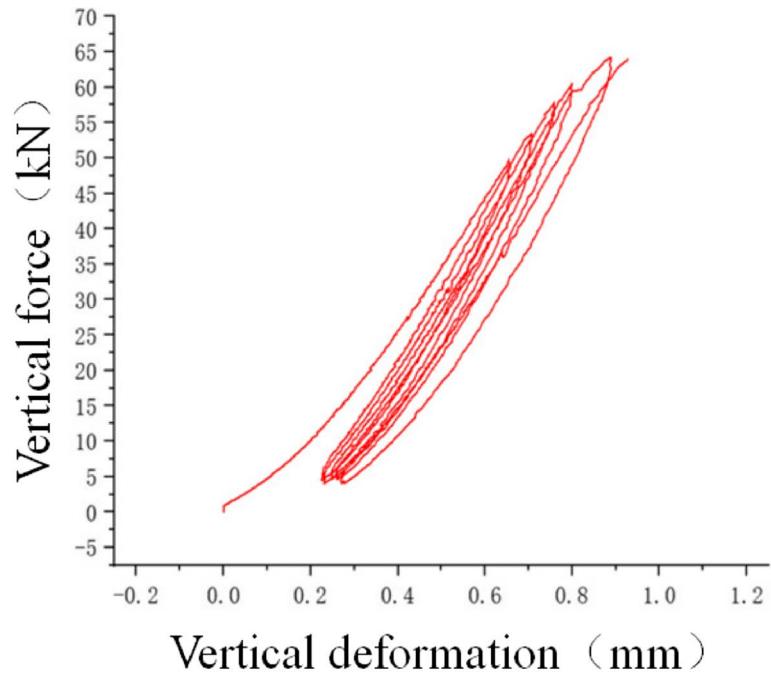
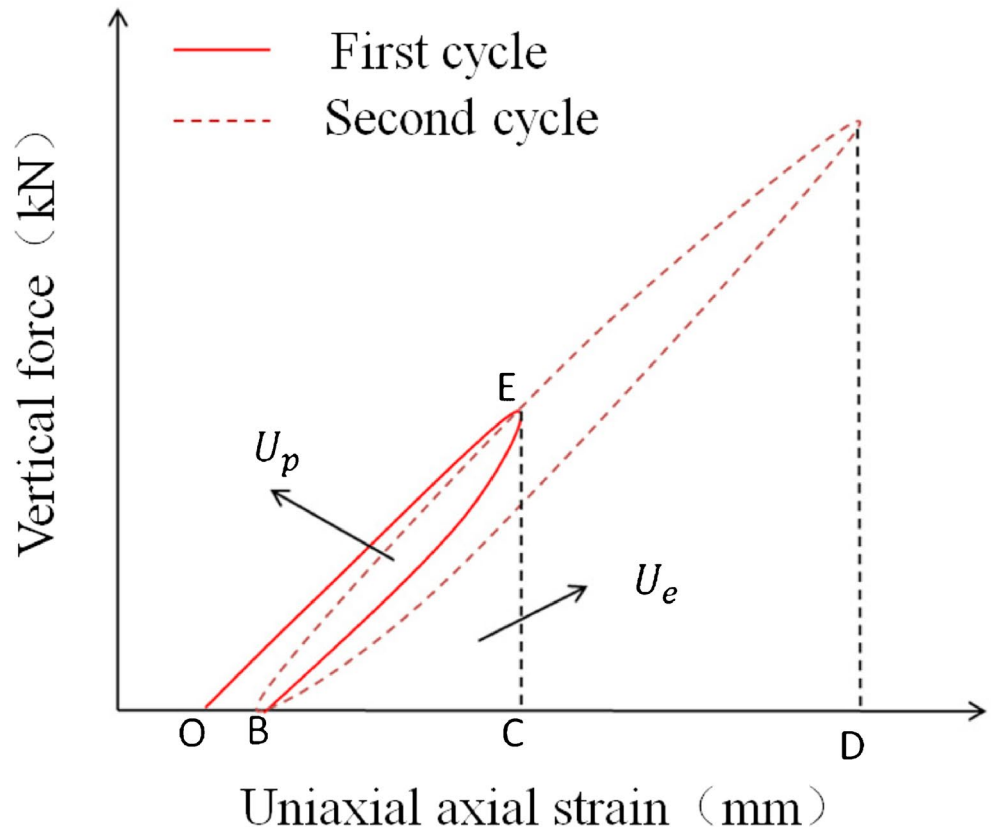


Fig. 7 Energy analysis model of coal-rock combination



(1)



(2)

Table 3 Energy density of coal-rock combination with different dip angles in different load stages

Types of specimens	Cycle progress numerical (kN)											
	5 kN	10 kN	15 kN	20 kN	25 kN	30 kN	35 kN	40 kN	45 kN	50 kN	55 kN	
0°	U	0.1431	0.3909	0.9792	1.4961	3.5653	5.5951	6.5702	7.5789	9.7311	11.3308	13.3987
	U_e	0.1302	0.3692	0.9377	1.4527	3.5219	5.5241	6.4863	7.4589	9.6083	11.0886	13.1485
	U_p	0.0129	0.0217	0.0415	0.0416	0.0434	0.071	0.0839	0.12	0.1228	0.2422	0.2502
15°	U	0.1378	0.2078	1.3511	1.6499	2.3909	3.2645	4.3858	5.0764	6.5167	7.5274	8.8158
	U_e	0.1184	0.1690	1.2931	1.5871	2.3121	3.1828	4.2841	4.9643	6.3995	7.3887	8.6319
	U_p	0.0194	0.0388	0.058	0.0628	0.0788	0.0817	0.1017	0.1121	0.1172	0.1387	0.1839
30°	U	0.1937	0.2731	0.5544	1.0335	1.8216	2.5809	3.7667	4.6945	6.2689		
	U_e	0.1547	0.2143	0.4822	0.9288	1.7049	2.4458	3.6245	4.5151	6.0088		
	U_p	0.039	0.0588	0.0772	0.1047	0.1167	0.1351	0.1421	0.1794	0.2601		
45°	U	0.2104	0.3029	0.7174	1.4106	2.0537	3.8728	5.0522				
	U_e	0.1868	0.2488	0.6570	1.3355	1.9757	3.7699	4.8324				
	U_p	0.0236	0.0541	0.0604	0.0751	0.078	0.1029	0.2198				
60°	U	0.3179	0.4277	1.0348	1.5726	2.8847	3.2826					
	U_e	0.2569	0.2906	0.8626	1.3937	2.6505	3.5867					
	U_p	0.061	0.1371	0.1722	0.1789	0.2342	0.2359					

the internal energy evolution process of coal-rock combination system, only reversible elastic energy is accumulated in the internal rock mass, and all plastic deformation energy and damage energy in the system are dissipated in the internal coal mass. According to the stress–strain curve of cyclic loading and unloading test of composite specimens, it can be seen from the diagram that the unloading curve does not coincide with the original loading path and is lower than the loading curve in the loading and unloading process of a cycle. Based on the stress–strain curve of a cycle in Fig. 6(b), the area under the curve OEC is the work U of the external load on the combination, the area under the curve BEC is the elastic energy U_e released by the combination during unloading, and the area contained in the curve OE and BE is the energy U_p dissipated inside the coal body.

Analysis of energy evolution law of inclined coal-rock combination

According to the curve model of a certain cycle stage in Fig. 6(b), the corresponding input energy and release energy can be calculated by using the formula, and then the dissipation energy can be obtained by subtracting the two. The main calculation formula is shown in the following equation:

$$\begin{cases} U = \int_0^c \sigma d\varepsilon \\ U_e = \int_B^C \sigma d\varepsilon \\ U_p = U - U_e \end{cases} \quad (5)$$

Table 4 Fitting equation of energy evolution during loading process of coal-rock combination

Test specimen number	Fitting equation of input energy density	Energy density fitting equation of elastic energy	Fitting equation of dissipative energy density
0°	$U = 0.0109\sigma^2 + 0.2049\sigma - 0.8843$ $R^2 = 0.9891$	$U_e = 0.0111\sigma^2 + 0.1977\sigma - 0.9098$ $R^2 = 0.9894$	$U_p = 7.60310^{-4}\sigma^2 - 0.0098\sigma + 0.0538$ $R^2 = 0.9599$
15°	$U = 0.0072\sigma^2 + 0.1283\sigma - 0.3381$ $R^2 = 0.9941$	$U_e = 0.006\sigma^2 + 0.1318\sigma - 0.4098$ $R^2 = 0.9952$	$U_p = 8.050910^{-5}\sigma^2 + 0.0029\sigma + 0.0208$ $R^2 = 0.9598, R^2 = 0.9622$
30°	$U = 0.0138\sigma^2 + 0.0559\sigma + 0.2118$ $R^2 = 0.9981$	$U_e = 0.0133\sigma^2 - 0.0509\sigma + 0.1287$ $R^2 = 0.9978$	$U_p = 3.130010^{-4}\sigma^2 + 0.0012\sigma + 0.00437$ $R^2 = 0.9474$
45°	$U = 0.2267\sigma^2 - 0.1395\sigma + 0.4251$ $R^2 = 0.9879$	$U_e = 0.0209\sigma^2 - 0.1089\sigma + 0.2539$ $R^2 = 0.9847$	$U_p = 9.196710^{-4}\sigma^2 - 0.0088\sigma + 0.0587$ $R^2 = 0.9548$
60°	$U = 0.0117\sigma^2 + 0.0458\sigma + 0.0236$ $R^2 = 0.9833$	$U_e = 0.0205\sigma^2 - 0.0742\sigma + 0.1455$ $R^2 = 0.9927$	$U_p = -8.011710^{-4}\sigma^2 + 0.0274\sigma + 0.0041$ $R^2 = 0.9598$

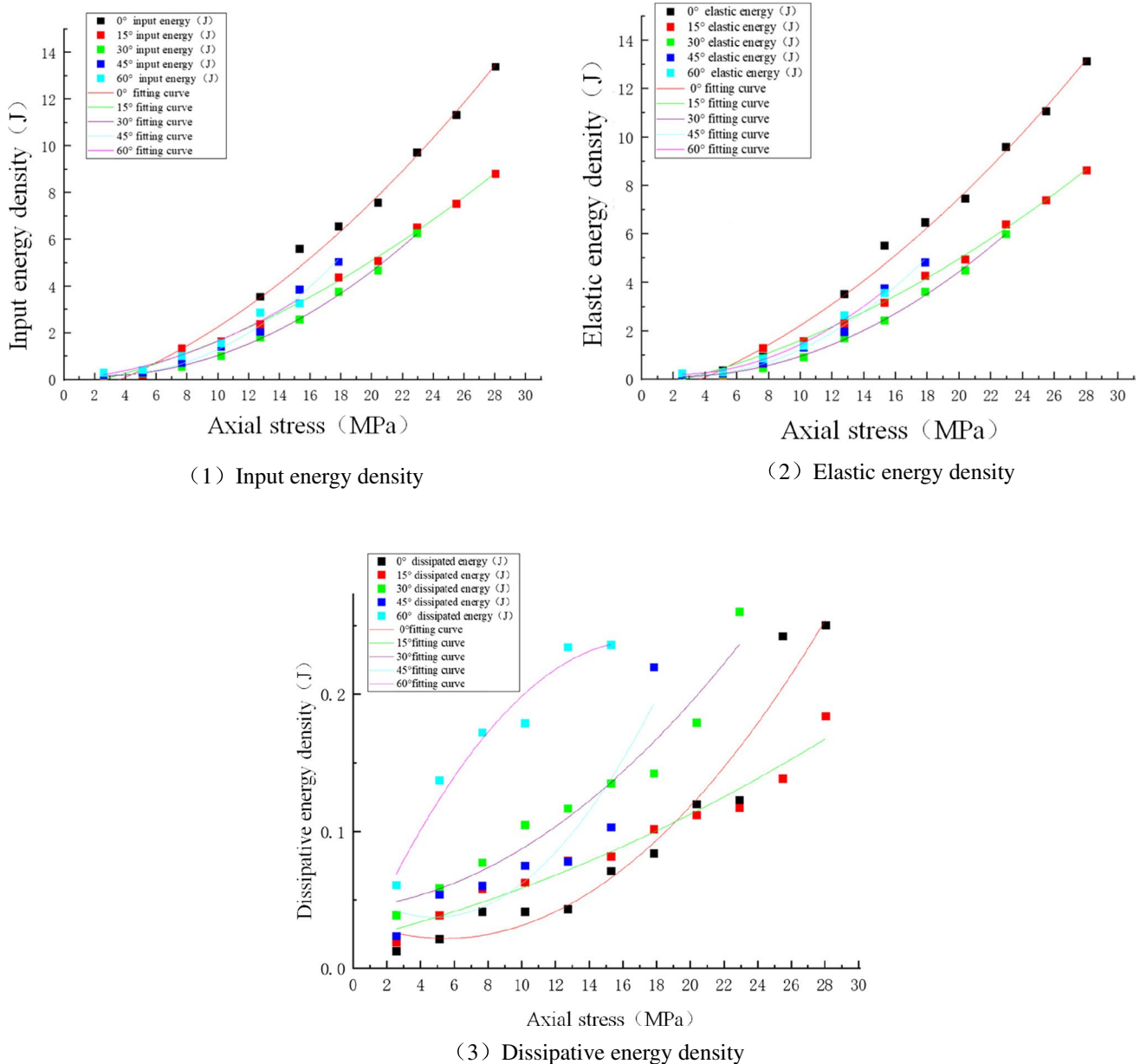


Fig. 8 Energy evolution fitting curve of coal-rock combination

The energy density of energy concentration, energy input, and energy dissipation under different loads in Fig. 7 are calculated by Eq. (5). The calculated data are arranged as follows:

The data trend of Table 3 is expressed by quadratic function relation (Table 4), and then the data is fitted. The fitting effect is significant, especially the correlation coefficient R^2 of input energy, and elastic energy density is about 0.9978. However, the correlation coefficient R^2 of the quadratic function fitting equation of

dissipation energy is about 0.9548, and the effect is poor. From the fitting curve of Fig. 8(a, b), it can be seen that the curves of the coal-rock combination always maintain a specific stable state during the compression process, and the curves have nonlinear evolution characteristics. However, the quadratic function fitting equation of the energy density curve of Fig. 8(c) is poor, but it also shows a nonlinear characteristic.

The energy change process in Fig. 9 drawn from each group of specimens' energy data in Table 3 is analyzed.

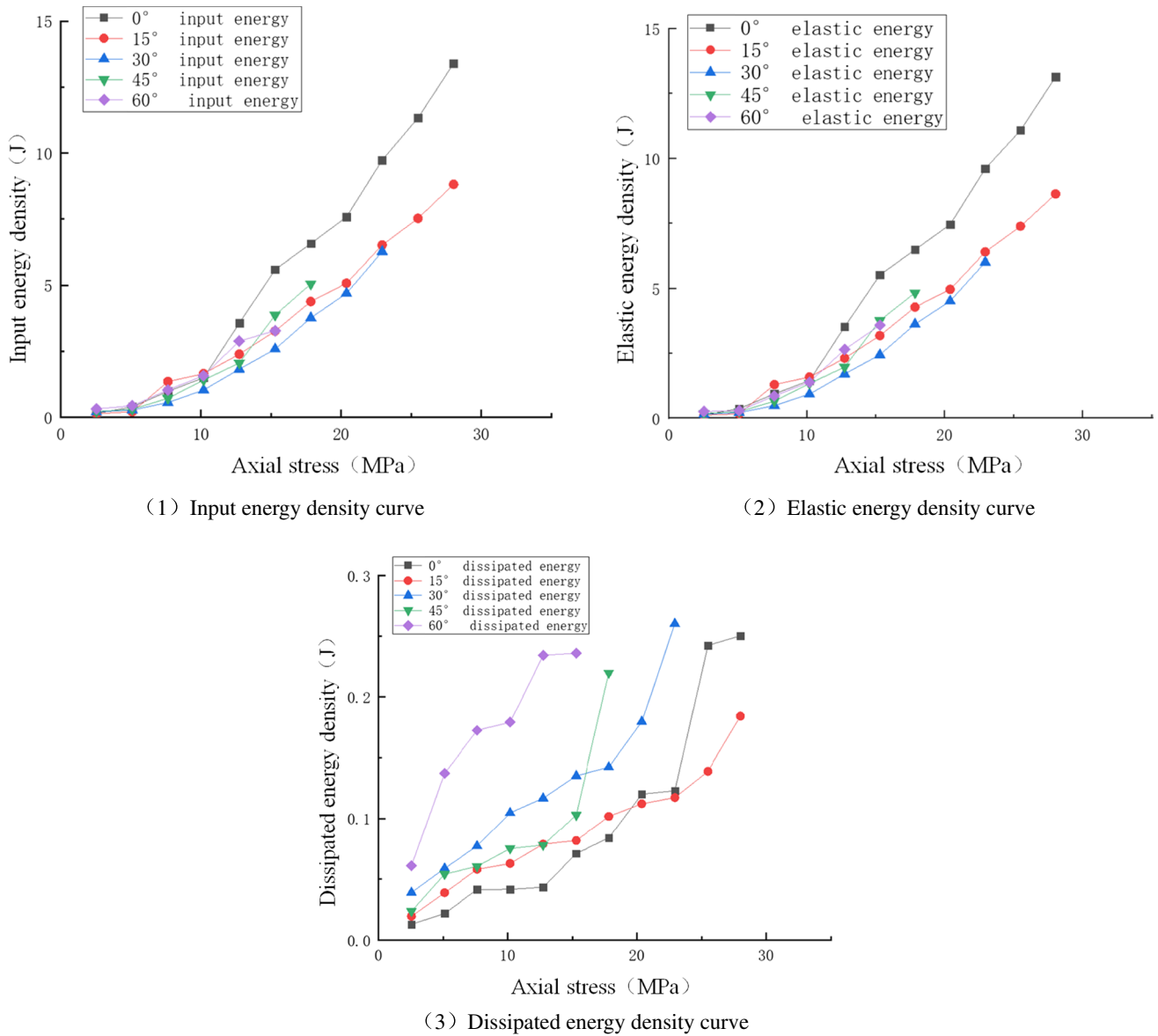


Fig. 9 The energy evolution process of the combination

In general, each specimen’s ultimate compressive strength decreases with the increases of coal dip angle, and the input energy density and the released elastic energy density of each group of specimens increase with the increase of peak load. This is due to the difference in material between coal and rock mass and the difference in damage degree between coal and rock mass after loading. When the composite is deformed under

compression, since the elastic modulus of sandstone is greater than that of coal, the axial strain and circumferential strain of sandstone at the same time are smaller than those of coal. Therefore, the rock mass begins to destroy after the coal body reaches destruction, so the degree of coal crushing is greater than that of the rock mass. This effect starts from the increase of the dip angle of the coal and rock mass; the greater the dip

angle of the coal and rock mass is, the more severe the coal crushing is, the more pronounced the crack is, and the main crack from the coal body through the rock mass are more significant.

It can be seen from Fig. 9(a, b) that the slow increase of the input energy density and elastic energy density of the coal-rock combination at the beginning of the cycle corresponds to the pore compaction stage in the compression process of the specimen. At this time, the input energy is close to elastic energy. This is because the specimen's input energy is stored in the interior of the specimen in the form of elastic energy after compression, and only a small part of the energy is dissipated. During the third cycle, the input energy and elastic energy density gradually increase when the specimen enters the elastic deformation stage. The elastic energy and input energy at 0° are significantly higher than those of other specimens. At this time, the coal and rock mass can withstand more energy input, and the dissipation energy consumption is less. The input energy and elastic energy of coal and rock mass with a dip angle of 60° increase with the load increase and the dissipation energy is faster than that of other dip angle combinations. It is urgent to pay attention to the point when mining coal and rock roadways with large dip angles.

Therefore, in the compression specimen, when the dissipative energy begins to release in the coal body with a large dip angle, the rock mass has not begun to release energy. The overall deformation of the coal body with a small dip angle is consistent, and the cracks develop and release less energy. When the inclination angle increases, the overall internal damage intensifies, which leads to the increase of the dissipation energy density of the coal mass of each component specimen with the increase of cyclic peak value (where the dissipation energy U_p in the first cycle is the accumulated dissipation energy of the coal mass in the process of loading the specimen from the initial load to the peak strength of 5 kN). The specimen's dissipation energy with a large inclination angle increases gradually in each cycle, and the rate is faster and faster. The dissipation energy of specimens with small inclination increases slowly in each cycle.

Conclusions

- (1) Compared with the composite's single-axial loading failure, the main failure mode mainly presents an *X*-type shear crack, whose failure is mainly concentrated in the coal part, and the coal is more fragmented dense. The ultimate failure strength is closer to the coal monomer's failure strength, and the fine and dense secondary cracks are dispersed along the main crack of the

coal body. The coal body's main crack runs through the rock mass, which is caused by the crack expansion after coal body failure.

- (2) During the loading process of coal-rock combination, the input energy, elastic energy, and dissipation energy in the pre-peak stage show prominent nonlinear growth characteristics with increased axial stress. From the energy density and stress curve, it can be seen that similar to the compaction section, elastic deformation section, and unstable fracture development stage in the compression process of the specimen, the elastic energy stored in the specimen during the whole development process is higher and the dissipation energy is less. When the specimen reaches the ultimate load, the dissipation energy begins to increase.
- (3) From the fitting of energy density data, it can be seen that the fitting effect is significant that the correlation coefficient R^2 of input energy and elastic energy density is about 0.9978. However, the correlation coefficient R^2 of the quadratic function fitting equation of dissipative energy is about 0.9548, and the effect is poor. It is found from the fitting curve that the curve of the coal-rock combination always maintains a certain stable state during the compression process, and the curve has nonlinear evolution characteristics.
- (4) The energy characteristics of coal-rock combination failure are as follows: during the compression process, the coal and rock mass begin to store elastic energy continuously, and the coal energy storage speed is fast. For the combination with a dip angle of 0° , the elastic energy and input energy are higher than those of other specimens. This is because coal and rock can withstand more energy input and consume less dissipated energy. For coal-rock mass with an inclination angle of 60° , the input energy and elastic energy decrease with the increase of load, and the dissipation energy is faster than that of other inclination combinations.

Acknowledgements We would like to thank the anonymous reviewers who have helped to improve the paper.

Funding This work was supported by the National Natural Science Foundation of China (No. 51974117, No. 52174076) and Hunan Natural Science Foundation Project (No. 2020JJ4027).

Declarations

Conflict of interest The authors declare no competing interests.

References

- Cai MF (2013) Rock mechanics and engineering[M]. Science Press, Beijing, pp 210–216
- Chen Y, Zuo JP, Song HP et al (2017) Energy nonlinear evolution characteristics of the failure behavior of coal-rock combined body[J]. *Chin J Undergr Space Eng* 13(1):125–132. <https://kns.cnki.net/kcms/detail/detail.aspx?FileName=BASE201701018&DbName=CJFQ2017>
- Chen Y, Zuo JP, Song HP et al (2018) Deformation and crack evolution of coal-rock combined body under cyclic loading-unloading effects[J]. *J Min Saf Eng* 35(4):826–833. <https://kns.cnki.net/kcms/detail/detail.aspx?FileName=KSYL201804022&DbName=CJFQ2018>
- Qin ZC, Zhou ST, Liu MQ (2015) Study on stability of surrounding rock in uphill mining stope with large inclination[J]. *Coal Eng* 47(7):86–88. <https://kns.cnki.net/kcms/detail/detail.aspx?FileName=MKSJ201507030&DbName=CJFQ2015>
- Qin ZC, Chen GB, Qin QJ (2017) Effects of combination mode on mechanical properties and rock burst tendency of the coal-rock combinations[J]. *J Xi'an Univ Sci Technol* 37(5):656–661. <https://kns.cnki.net/kcms/detail/detail.aspx?FileName=XKXB201705009&DbName=CJFQ2017>
- Shi JJ, Shi HY, Bao SS et al (2012) The hydraulic support parameter design in lean coal seam and numerical simulation about the relation hydraulic support and surround rock[J]. *J China Coal Soc* 37(supp.2):314–318. <https://kns.cnki.net/kcms/detail/detail.aspx?FileName=MTXB2012S2010&DbName=CJFQ2012>
- Xiao FK, Shen ZL, Liu G et al (2014) Relationship between hysteresis loop and elastoplastic strain energy during cyclic loading and unloading[J]. *Chin J Rock Mech Eng* 33(9):1792–1797. <https://kns.cnki.net/kcms/detail/detail.aspx?FileName=YSLX201409009&DbName=CJFQ2014>
- Xie HP, Zhou HW, Xue DJ et al (2012) Research and consideration on deep coal mining and critical mining depth[J]. *J China Coal Soc* 37(4):535–542. <https://kns.cnki.net/kcms/detail/detail.aspx?FileName=MTXB201204002&DbName=CJFQ2012> (in Chinese)
- Xu J, Xian XF, Wang H et al (2006) Experimental study on rock deformation characteristics under cycling loading and unloading conditions[J]. *Chin J Rock Mech Eng* 25(Supp.1): 3040–3045. <https://kns.cnki.net/kcms/detail/detail.aspx?FileName=YSLX2006S1067&DbName=CJFQ2006>
- Xu J, Zhang Y, Yang HW et al (2011) Energy evolution law of deformation and damage of sandstone under cyclic pore water pressures[J]. *Chin J Rock Mech Eng* 30(1):141–148. <https://kns.cnki.net/kcms/detail/detail.aspx?FileName=YSLX201101014&DbName=CJFQ2011>
- Yang L, Gao FQ, Liu HL et al (2019) Energy evolution law and failure mechanism of coal-rock combined specimen[J]. *J China Coal Soc* 44(12):3895–3902. <https://kns.cnki.net/kcms/detail/detail.aspx?FileName=MTXB201912032&DbName=CJFQ2019>
- Yu WJ, Li K (2020) Deformation mechanism and control technology of surrounding rock in the deep-buried large-span chamber[J]. *Geofluids* 2020(1):1–22. <https://doi.org/10.1155/2020/8881319>
- Yu WJ, Wu GS, Liu H et al (2018) Deformation characteristics and stability control of soft coal-rock mining roadway in thin coal seam [J]. *J China Coal Soc* 43(10):2668–2678. <https://kns.cnki.net/kcms/detail/detail.aspx?FileName=MTXB201810002&DbName=CJFQ2018> (in Chinese)
- Yu WJ, Pan B, Zhang F et al (2019a) Deformation characteristics and determination of optimum supporting time of alteration rock mass in deep mine [J]. *KSCE J Civ Eng* 23(11):4921–4932. <https://doi.org/10.1007/s12205-019-0365-y>
- Yu WJ, Wu GS, An BF et al (2019b) Experimental study on the brittle-ductile response of a heterogeneous soft coal rock mass under multifactor coupling [J]. *Geofluids* 1–15. <https://doi.org/10.1155/2019/5316149>
- Yu WJ, Wu GS, Liu Z et al (2019c) Experimental study on uneven failure of loose coal and rock composite specimen[J]. *Coal Sci Technol* 47(1): 85–90. <https://kns.cnki.net/kcms/detail/detail.aspx?FileName=MTKJ201901047&DbName=CJFQ2019>
- Yu WJ, Wu GS, Liu Z et al (2020) Uniaxial compression test of coal-rock-bolt anchorage body and mechanical mechanisms of bolts[J]. *Chin J Rock Mech Eng* 39(1):57–68. <https://kns.cnki.net/kcms/detail/detail.aspx?FileName=YSLX202001006&DbName=DKFX2020>
- Yu WJ, Wu GS, Pan B et al (2021) Experimental investigation of the mechanical properties of sandstone-coal-bolt specimens with different angles under conventional triaxial compression. *Int J Geomech*. [https://doi.org/10.1061/\(ASCE\)GM.1943-5622.0002005](https://doi.org/10.1061/(ASCE)GM.1943-5622.0002005). <https://ascelibrary.org/doi/10.1061/%28ASCE%29GM.1943-5622.0002005>
- Zhang B, Cao SG, Wang LG et al (2011) Deformation failure mechanism and support measurements in roadway of steeply inclined coal seam[J]. *J Min Saf Eng* 28(2):215–219. <https://kns.cnki.net/kcms/detail/detail.aspx?FileName=KSYL201102010&DbName=CJFQ2011>
- Zhao HL, Zhao Y (2018) Influence of dip angle of coal and rock combination on outburst tendency based on particle flow code [J]. *Saf Coal Mines* 49(3):198–201. <https://kns.cnki.net/kcms/detail/detail.aspx?FileName=MKAQ201803053&DbName=CJFQ2018>
- Zheng JB, Wang QZ, Yang S et al (2015) Surrounding rock deformation and stability control technology of roadway influenced by repeating mining[J]. *Coal Min Technol* 20(3):76–80. <https://kns.cnki.net/kcms/detail/detail.aspx?FileName=MKAQ201803053&DbName=CJFQ2018>
- Zhu ZH, Feng T, Gong FQ et al (2016) Experimental research of mechanical properties on grading cycle loading-unloading behavior of coal-rock combination bodies at different stress levels[J]. *J Cent South Univ (Sci Technol)* 47(7):2470–2475. <https://kns.cnki.net/kcms/detail/detail.aspx?FileName=ZNGD201607039&DbName=CJFQ2016>
- Zuo JP, Xie HP, Wu AM et al (2011a) Investigation on failure mechanisms and mechanical behaviors of deep coal-rock single body and combined[J]. *Chin J Rock Mech Eng* 30(1):85–92. <https://kns.cnki.net/kcms/detail/detail.aspx?FileName=YSLX201101009&DbName=CJFQ2011>
- Zuo JP, Xie HP et al (2011b) Experimental research on loading-unloading behavior of coal -rock combination bodies at different stress levels[J]. *Rock Soil Mech* 32(5):1288–1296. <https://kns.cnki.net/kcms/detail/detail.aspx?FileName=YTLX201105002&DbName=CJFQ2011>
- Zuo JP, Chen Y, Zhang JW et al (2016) Failure behavior and strength characteristics of coal-rock combined body under different confining pressures[J]. *J China Coal Soc* 41(11):2706–2713. <https://kns.cnki.net/kcms/detail/detail.aspx?FileName=MTXB201611007&DbName=CJFQ2016>